AJNR

Warthin tumor of the parotid gland: MR-pathologic correlation.

M Minami, H Tanioka, K Oyama, Y Itai, M Eguchi, K Yoshikawa, T Murakami and Y Sasaki

AJNR Am J Neuroradiol 1993, 14 (1) 209-214
http://www.ajnr.org/content/14/1/209

Warthin Tumor of the Parotid Gland: MR-Pathologic Correlation

Manabu Minami,[1,6] Hisaya Tanioka,[4] Kazuyuki Oyama,[1] Yuji Itai,[1,3] Masanobu Eguchi,[5] Kohki Yoshikawa,[4] Toshikazu Murakami,[2] and Yasuhito Sasaki[1]

PURPOSE: To describe the MR appearance of Warthin tumor and correlate the images with pathologic sections. **METHODS:** MR studies of seven patients with Warthin tumors in the parotid gland were retrospectively reviewed; MR results were compared with pathologic specimens in five instances. **FINDINGS:** One patient had a bilateral tumor; another had three tumors in the right parotid gland and one in the left. Ten tumors showed well-defined borders; the other, which was accompanied by infection, had an indefinite border only at the upper pole. All had thin capsules not shown on MR. Four showed small lobulations at the margins. Fibrosis appeared as septa-like structures of low signal intensity in three cases. There were areas of hemorrhage with accumulation of hemosiderin in two cases. All tumors had low or intermediate T1-weighted signal intensity, four with high intensity areas of cysts containing cholesterol crystals. On T2W images, two tumors had homogeneously intermediate intensity; the other nine had mixed intensity. Areas of intermediate intensity were correlated with abundant epithelial tissues; focal high-intensity areas were correlated with cysts and/or areas of predominant lymphoid proliferation. **CONCLUSIONS:** MR findings such as bilaterality and/or multiplicity, well-defined margins, and predominantly intermediate signal intensity on T1W and T2W images with focal areas of high signal intensities on T1W images suggest Warthin tumor, but are not pathognomonic.

Index terms: Salivary glands, neoplasms; Salivary glands, magnetic resonance; Warthin tumor; Neck, magnetic resonance

AJNR 14:209–214, Jan/Feb 1993

Warthin tumors (adenolymphoma, papillary cystadenoma lymphomatosum, lymphomatous adenoma) are benign entities that account for 5% to 10% of tumors in the parotid gland. They are much more common in men than in women (the ratio is 5 to 1), especially men of middle-age (40 to 70 years old). In about 5% to 10% of cases they are bilateral; they may also be multiple in the unilateral gland. Some authors have described magnetic resonance (MR) findings of this entity among series of parotid lesions, but descriptions concerning signal intensities of the tumor are variable: on T2-weighted (T2W) images, some are high (2–6), while others are similar in intensity to the normal parotid gland (3, 4, 7, 8); some are homogeneous (3, 4, 6, 8–10), while others are heterogeneous (3, 4, 6, 9). In this study, we review MR findings of Warthin tumors and correlate them with pathologic findings to elucidate the variability of MR findings.

Methods and Materials

We reviewed MR studies of the parotid gland in seven patients with pathologically proved Warthin tumor. The patients, six men and one woman, had a mean age of 63 years (47–73 year range). All had undergone surgery and pathologic examination; no needle biopsies had been performed prior to surgery. All MR examinations were performed using 1.5-T MR units. In two cases, a ring-type

Received June 28, 1991; revision requested November 16; revision received March 6, 1992 and accepted July 3.

This paper was presented at the 76th Scientific Assembly and Annual Meeting of the RSNA in Chicago, November 16, 1990.

[1] Department of Radiology, (M.M., K.O., Y.I., Y.S.) University of Tokyo Hospital, Tokyo, Japan.

[2] Department of Pathology (T.M.), University of Tokyo Hospital, Tokyo, Japan.

[3] Department of Radiology (Y.I.), University of Tsukuba Hospital, Tsukuba, Japan.

[4] Department of Radiology (H.T., K.Y.) Kanto Rosai Hospital, Kawasaki, Japan.

[5] Department of Pathology, Kanto Rosai Hospital, Kawasaki, Japan.

[6] Address reprint requests to M. Minami, Department of Radiology, University of Tokyo Hospital, 7-3-1 Hongo, Bunkyo-ku, Tokyo 113, Japan.

AJNR 14:209–214, Jan/Feb 1993 0195-6108/93/1401-0209

surface coil was used: contiguous sagittal T1-weighted (T1W) images with a section thickness of 4 mm were obtained using spin-echo sequences of 600/15–22/4 (TR/TE/excitations); contiguous coronal T2W images with a section thickness of 4 mm were obtained using spin-echo pulse sequences of 1600–2500/80–90/2. In the other five cases, a head coil was used: multiple axial T1W images with section thickness of 5 mm and 6-mm intervals were obtained using spin-echo sequences of 500–600/15–17/2; axial T2W images in the same position as T1W images were obtained with sequences of 1600–3000/90/1. Coronal or sagittal T1W images were occasionally obtained for further evaluation.

Three radiologists evaluated the images (M.M., H.T., K.O.) to determine the bilaterality and multiplicity, location (superficial lobe or deep lobe), nature of the margin (sharpness and lobulation), internal architecture (septa and hemorrhage), and signal intensities of the tumors. Areas of high T1W and low T2W signal intensities were considered to be hemorrhage. The signal intensity of tumors was compared with that of fat (high intensity) and muscle (low intensity) on T1W images, and with that of cerebrospinal fluid (high intensity), normal portions of the parotid gland (intermediate intensity), and muscle (low intensity) on T2W images. In the cases in which a surface coil had been used, signal intensities were compared at the same depth from the skin surface.

Pathologic specimens were reviewed both grossly and microscopically in five cases. The sections were correlated with the MR images as closely as possible by one radiologist (M.M.) and two pathologists (M.E., T.M.). The iron staining method using the Berlin-blue reaction was also employed in three tumor specimens.

Results

Eleven tumors with mean diameter of 2.3 cm (range, 0.7–3.2 cm) were found in seven cases. In one case, there was one bilateral tumor; in another, there were three tumors in the right parotid gland and one in the left. Eight tumors were located in the right parotid gland, three in the left. Nine of the tumors were situated in the superficial lobe; the others were in the deep lobe of the parotid gland. Ten tumors showed well-defined margins (Figs. 1-3); the other revealed an indefinite border at the upper pole of the tumor, with well-defined borders elsewhere. Four tumors showed small lobulations at the margins. In three cases, there were septa-like structures, which had low T1W and low T2W signal intensities. In two cases, there were areas considered to be hemorrhage (Fig. 3).

On T1W images, all the tumors had low or intermediate signal intensity; however, four of them also showed multiple high-intensity areas on T1W images (Figs. 1 and 3). On T2W images, two tumors had homogeneously intermediate intensity, both in the patient with four tumors. The other nine tumors appeared on T2W images as lesions of mixed intensity; that is, intermediate intensity with focal high intensity regions (Figs. 1 and 3). High intensity areas were small in four of the nine tumors (Figs. 2 and 3). In five of the nine tumors, high intensity areas of irregular thickness were predominantly observed in the periphery of the tumors (Figs. 1 and 2).

Radiologic pathologic correlations revealed the following findings. All tumors had thin capsules that were not demonstrated by MR. One tumor with an indefinite border on MR images was accompanied by infection. Septa-like structures on MR images were ascertained to be fibrosis (Fig. 1B). Two tumors had localized hemorrhage demonstrated by MR; the Berlin-blue staining of one showed corresponding focal accumulation of hemosiderin.

High-intensity areas on T1W images corresponded to cysts containing proteinaceous fluids with cholesterol crystals or foamy cells (Figs. 1B and 3C). Cysts with scanty cholesterol crystals appeared as hypointense as or slightly more hypointense than the tumors themselves on T1W images. Intermediate intensity areas on T2W images were correlated with abundant epithelial tissues (Fig. 2C), while focal high-intensity areas were correlated with cysts and/or areas of predominant lymphoid proliferation (Fig. 3C). Predominant high-intensity areas in the periphery of tumors on T2W images were thought to be rich proliferations of reactive lymphocytes in the subcapsular regions, surrounding the epithelial portions in the center (Fig. 2C). Iron staining was not diffuse but focal even in areas of hemorrhage; therefore, the cause of intermediate signal intensity on T2W images was not considered to be the accumulation of hemosiderin.

Discussion

Warthin tumors are grossly ovoid and have a smooth surface. Most Warthin tumors vary from partly to predominantly cystic; the cyst fluid, which is usually brown and tenacious, may be yellow and thin with cholesterol crystals in some cases (1). Cyst formation is reported in about 30% of cases (1). This entity should be suspected when MR or computed tomography (CT) shows a mass of well-defined smooth margins, cyst formation, and bilaterality or multiplicity (12, 13). In the parotid glands, however, these findings are

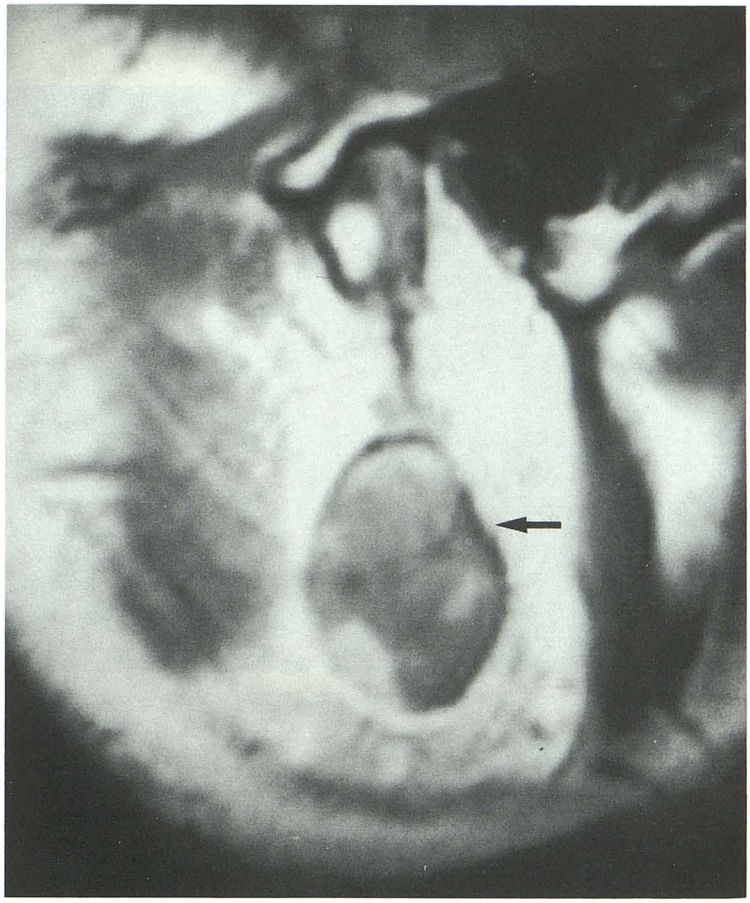

A

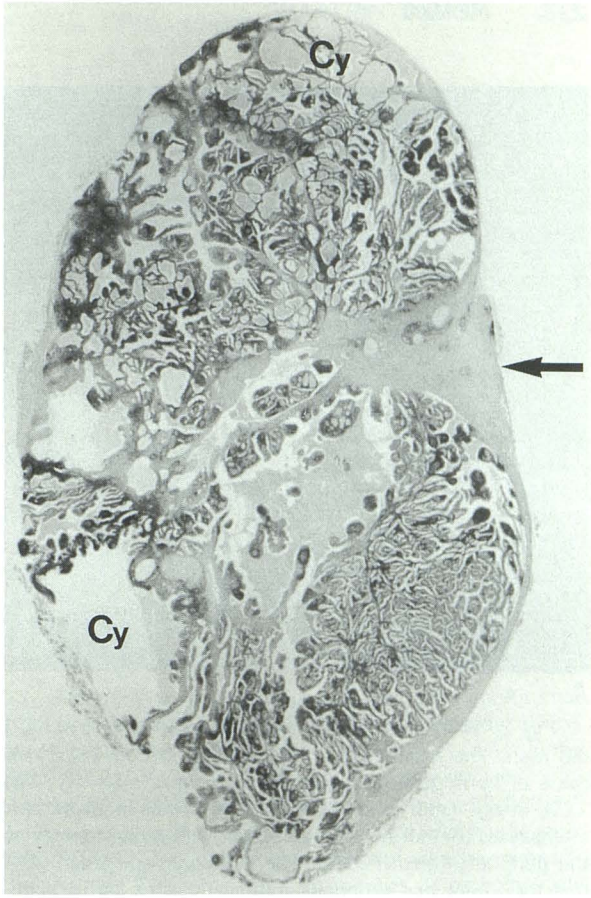

B

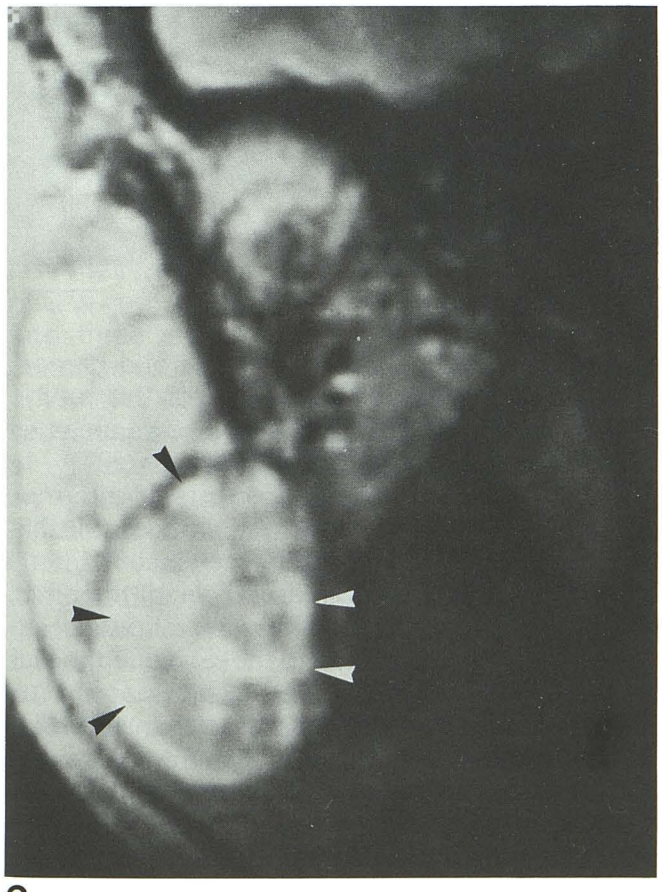

C

Fig. 1. Warthin tumor in the right parotid gland of a 47-year-old man. The sagittal T1W image (spin echo 600/17, *A*) shows a well-defined tumor of intermediate intensity, with multiple high-intensity areas. A fan-shaped area of lower intensity is seen at the periphery of the tumor (*arrow*). A sagittal section of the specimen (*B*) proves that the multiple high-intensity areas are cysts containing rich, foamy cells (*Cy*) and that the lower intensity area corresponds to fibrosis (*arrow*). The coronal T2W image (spin echo 2500/80, *C*) shows the intermediate intensity mass with focal high-intensity areas, especially in the periphery (*arrowheads*).

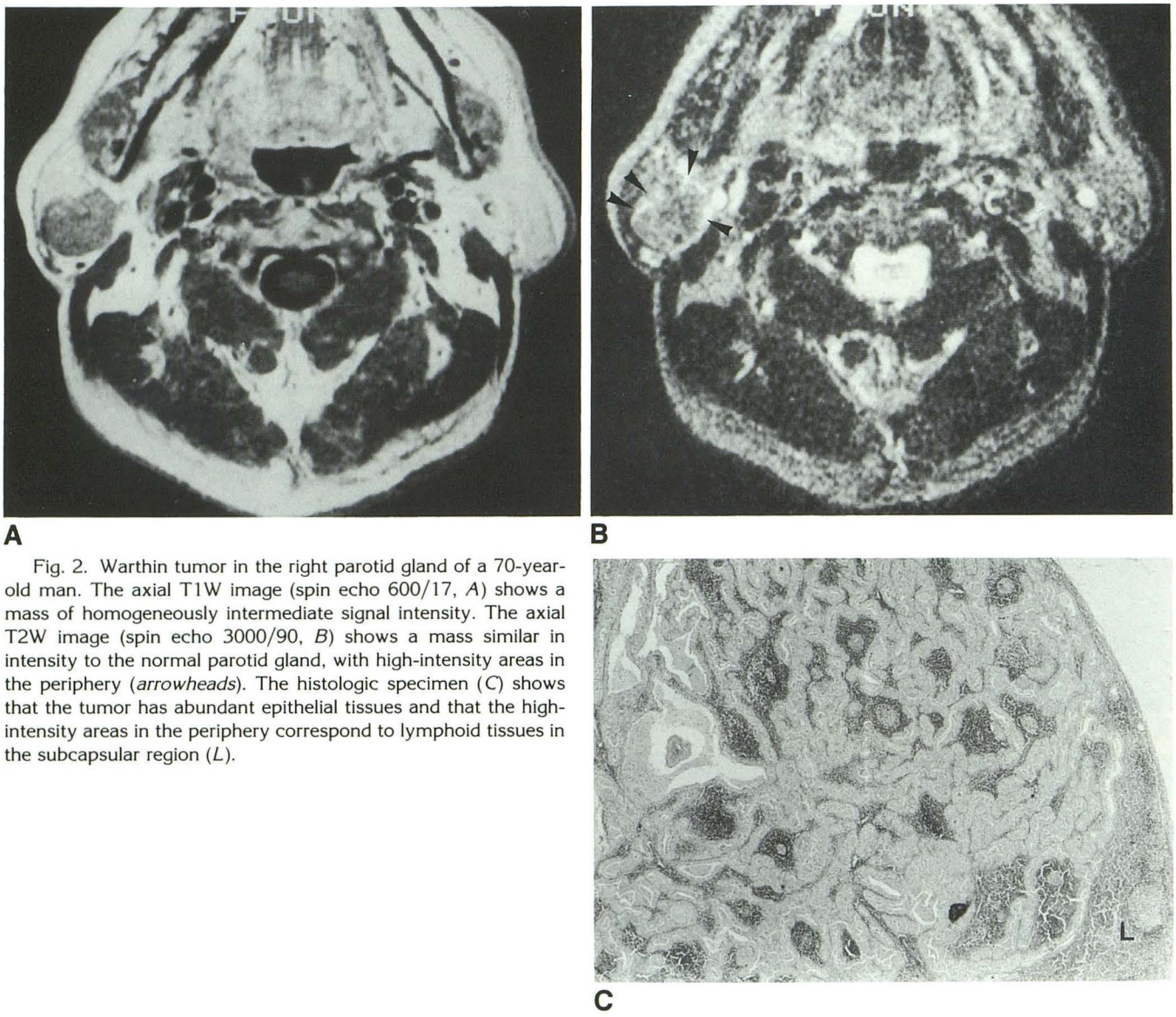

A B C

Fig. 2. Warthin tumor in the right parotid gland of a 70-year-old man. The axial T1W image (spin echo 600/17, *A*) shows a mass of homogeneously intermediate signal intensity. The axial T2W image (spin echo 3000/90, *B*) shows a mass similar in intensity to the normal parotid gland, with high-intensity areas in the periphery (*arrowheads*). The histologic specimen (*C*) shows that the tumor has abundant epithelial tissues and that the high-intensity areas in the periphery correspond to lymphoid tissues in the subcapsular region (*L*).

not specific to Warthin tumor; any well-defined tumor is likely to be benign. Cyst formation can be seen in some inflammatory diseases, HIV-positive lymphoepithelial cyst, and other tumors, like pleomorphic adenoma. Bilateral lesions and multiple lesions in a single parotid gland can occur in inflammation (including autoimmune diseases and granulomatous diseases), intraparotid lymphadenopathy, oncocytoma, acinar cell carcinoma and other infiltrative malignant tumors, and, rarely, neurofibromatosis, lymphoid neoplasms, and metastasis (12, 14). In the present study, cysts containing cholesterol crystals appeared on T1W images as high-intensity areas; this finding may be suggestive of Warthin tumor, but hemorrhagic cysts or necrosis with proteinaceous fluid in other tumors like pleomorphic adenoma can show a similar pattern. Intraparotid hemorrhage was observed in two cases of this study; Swartz et al state that MR often shows areas of hemorrhage in cases of Warthin tumor (11).

Warthin tumors had components of intermediate signal intensity on T2W images in this series; two tumors showed homogeneous intensity similar to the normal parotid gland; the other nine showed mixed intensity. This difference in appearance was attributed to the ratio of epithelial tissue to lymphoid tissue and cystic spaces. Tumors isointense to the gland were rich in epithelial tissue, while hyperintense lesions were mixed with epithelial tissue, lymphoid proliferation, and cystic formation. This pattern recalls the various scintigraphic appearances of Warthin tumor obtained in a technetium-99m pertechnetate study

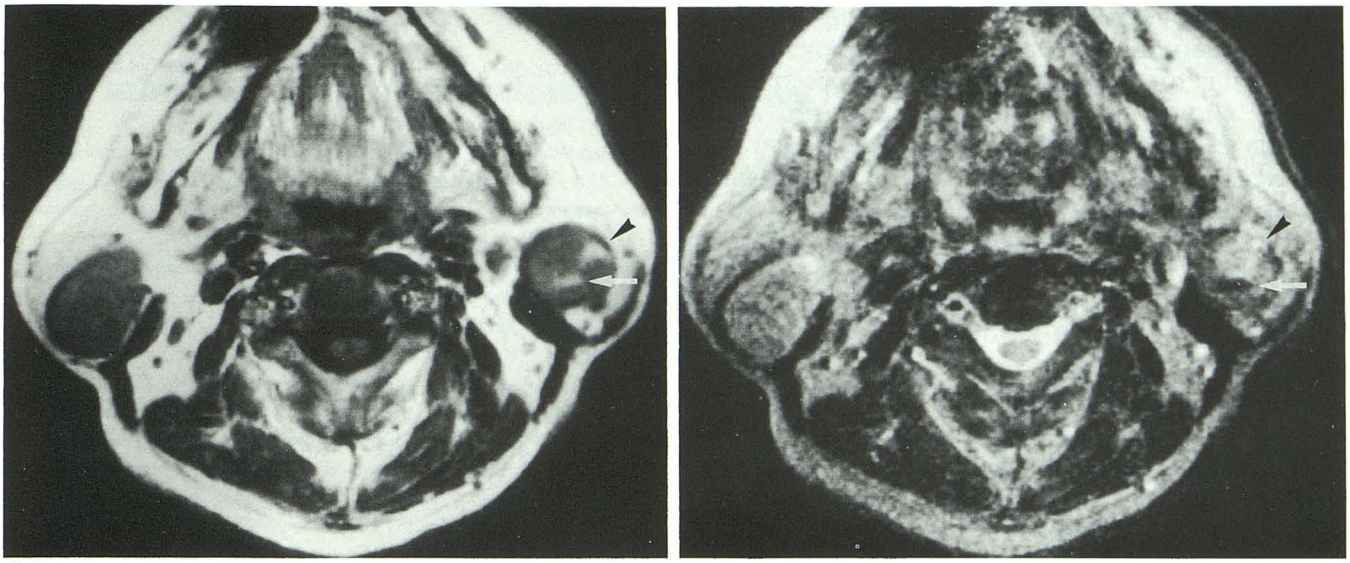

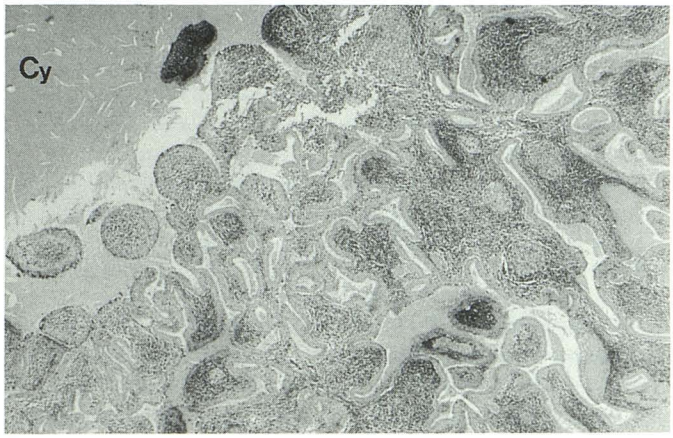

Fig. 3. Bilateral Warthin tumors of a 71-year-old man. A tumor in the right parotid gland shows low T1W and intermediate T2W signal intensities similar to the tumor of Figure 2. A tumor in the left parotid gland is revealed as a slightly low-intensity mass with high-intensity areas on the axial T1W image (spin echo 600/17, *A*) and a mass of mixed intensity on the axial T2W image (spin echo 3000/90, *B*). The anterior high-intensity area (*arrowhead*), which is larger on T2W than on T1W images, is pathologically correlated with cysts and areas of lymphoid proliferation (*C*). The cysts contain cholesterol crystals (*Cy*). The posterior high-intensity area on T1W images (*arrow*) was low in intensity on T2W images and was shown to be hemorrhage.

(15). Seifert et al carried out a pathologic review of 275 cases of Warthin tumor and divided them into three subtypes according to the ratio of epithelial tissue to lymphoid stroma (16): subtype 1 involves typical cystadenolymphoma (CAL), with an epithelial tumor component of 50% (77% of all cases); subtype 2, stroma-poor CAL, with an epithelial tumor component of 70% to 80% (13.5% of all cases); and subtype 3, stroma-rich CAL, with an epithelial tumor component of only 20% to 30% (2% of all cases). They postulate that Warthin tumors evolve from subtype 3 through subtype 1 to subtype 2 by further adenomatous epithelial proliferation.

We think Warthin tumors of subtype 2 are revealed as masses of intermediate intensity by MR, while those of subtype 1 or 3 are revealed as masses of inhomogeneous intensity. In their series, 75% of multifocal occurrence was observed in subtype 2; this was also observed in our series. We do not know the cause of intermediate signal intensity in areas dominated by epithelial tissue. Iron staining in the present study indicates that the low signal is not due to hemorrhage. Perhaps it reflects the hypercellularity of epithelial tissues with lack of fluid, as in cases of high-grade malignancies (5). However, epithelial tissues usually surround cystic spaces in Warthin tumors. Some paramagnetic substances might exist in mitochondria-rich epithelial tissues in Warthin tumors (1), but further research on this point will be necessary.

In the MR differential diagnosis of parotid lesions with low T1W and low T2W signal intensities, Som et al include high-grade malignancies (mucoepidermoid carcinoma, adenocarcinoma, undifferentiated carcinoma, and carcinoma ex-pleomorphic adenoma), fibrosis due to prior surgery or postoperative irradiation, vascular flow voids, and calcifications (5). Others have reported

that, besides Warthin tumor, pleomorphic adenoma, squamous cell carcinoma, adenoid cystic carcinoma, metastasis, lymphoma, and inflammation show relatively low-intensity on T2W images (3, 6, 8). Oncocytoma should also be included because of its similar histology with subtype 2 Warthin tumor. The exclusion of vascular flow voids and calcifications is not difficult radiologically (5). Ill-defined lesions such as inflammations and infiltrative malignancies are distinguishable from Warthin tumors, but not from severely infected ones.

The most difficult diagnostic problem is presented by fairly well-defined lesions of lower T2W signal intensity. In our experience, if the lesion has large lobulations, it is more likely to be pleomorphic adenoma or carcinoma expleomorphic adenoma; otherwise, differentiation on the basis of MR findings alone is difficult, necessitating scintigraphic studies using technetium-99m pertechnetate or needle biopsies. The sensitivity of radioisotope scanning is reported to be about 67% (17) and its spatial resolution is lower than that of MR or CT; however, one author reported that, on postdischarge images, Warthin tumors greater than 2 cm in diameter could be seen as hot lesions (15). Moreover, this examination is occasionally positive for carcinoma, oncocytoma, pleomorphic adenoma, and neurofibroma (18).

In conclusion, the current series shows that various MR findings correlated well with pathologic findings in Warthin tumor. Bilaterality and/or multiplicity, well-defined margins, and predominantly intermediate signal intensity on T1W and T2W images with focal areas of high signal intensities on T1W images suggest Warthin tumor. However, these findings are not pathognomonic and high-grade malignancies with well-defined margins make MR differentiation most problematic.

References

1. Thackray AC, Lucas RB. Adenolymphoma. In: *Tumors of the major salivary glands. Atlas of tumor pathology*, 2nd series, fasc 10. Washington, DC: AFIP, 1974:40–55
2. Mandelblatt SM, Braun IF, Davis PC, Fry SM, Jacobs LH, Hoffman JC Jr. Parotid masses; MR imaging. *Radiology* 1987;163:411–414
3. Casselman JW, Mancuso AA. Major salivary gland masses: comparison of MR imaging and CT. *Radiology* 1987;165:183–189
4. Anzai Y, Uno K, Nawano, et al. MR imaging of parotid masses. (abstr in English) *Jpn J Clin Radiol* 1988;33:1537–1541
5. Som PM, Biller HF. High-grade malignancies of the parotid gland: identification with MR imaging. *Radiology* 1989;173:823–826
6. Swartz JD, Rothman MI, Marlowe FI, Berger AS. MR imaging of parotid mass lesions: attempts at histopathologic differentiation. *J Comput Assist Tomogr* 1989;13:789–796
7. Mikulis DJ, Chisin R, Wismer GL, et al. Phase-contrast imaging of the parotid region. *AJNR* 1989;10:157–164
8. Vogl TJ, Dresel SJ, Spath M, et al. Parotid gland: plain and Gadolinium enhanced MR imaging. *Radiology* 1990;177:667–674
9. Schaefer SD, Maravilla KR, Close LG, Burns DK, Merkel MA, Suss RA. Evaluation of NMR versus CT for parotid masses: a preliminary report. *Laryngoscope* 1985;95:945–950
10. Teresi LM, Lufkin RB, Wortham DG, Abemayor E, Hanafee WN. Parotid masses: MR imaging. *Radiology* 1987;163:405–409
11. Chaudhuri TK, Stadalnik RC. Gamuts: salivary gland imaging. *Semin Nucl Med* 1980;10:400–401
12. Dillon WP, Mancuso AA. The oropharynx and nasopharynx. In: Newton TH, Hasso AN, Dillon WP, eds. *Computed tomography of the head and neck*. New York: Raven, 1988:10.53–10.60
13. Mancuso AA, Hanafee WN. Salivary glands. In: *Computed tomography and magnetic resonance imaging of head and neck*. 2nd ed. Baltimore: Williams & Wilkins, 1985:139–160.
14. Shugar JMA, Som PM, Biller HF. Warthin's tumor, a multifocal disease. *Ann Otol Rhinol Laryngol* 1982;91:246–249
15. Sostre S, Medina L, de Arellano GR. The various scintigraphic patterns of Warthin's tumor. *Clin Nucl Med* 1987;8:620–626
16. Seifert G, Bull HG, Donath K. Histologic subclassification of the cystadenolymphoma of the parotid gland: analysis of 275 cases. *Virchows Arch A Pathol Anat Histol* 1980;388:13–38
17. Shall GL. The role of radionuclide scanning in the evaluation of neoplasms of the salivary glands: a review. *J Surg Oncol* 1971;3:699–714
18. Silberstein EB. Salivary glands. In: Silberstein EB, McAfee JG, eds. *Differential diagnosis in nuclear medicine*. New York: McGraw-Hill, 1984;145–148